



## Influence of geomagnetic effects on large scale anisotropy searches

MORITZ MÜNCHMEYER<sup>1</sup> FOR THE PIERRE AUGER COLLABORATION<sup>2</sup>

<sup>1</sup>Laboratoire de Physique Nucléaire et de Hautes Energies, Universités Paris 6 et Paris 7, CNRS-IN2P3, Paris, France

<sup>2</sup>Observatorio Pierre Auger, Av. San Martín Norte 304, 5613 Malargüe, Argentina

(Full author list: [http://www.auger.org/archive/authors\\_2011\\_05.html](http://www.auger.org/archive/authors_2011_05.html))

[auger\\_spokespersons@fnal.gov](mailto:auger_spokespersons@fnal.gov)

**Abstract:** We discuss the influence of the geomagnetic field on the energy estimate of extensive air showers with zenith angles smaller than  $60^\circ$ , detected with the Surface Detector array of the Pierre Auger Observatory. The geomagnetic field induces a modulation of the energy estimator, depending on the shower direction, at the  $\sim 2\%$  level at large zenith angles. We present a method to account for this modulation in the reconstruction of the energy of the cosmic rays. We analyse the effect of the energy shift on large scale anisotropy searches in the arrival direction distributions of cosmic rays above the energy threshold at which the detection efficiency of the surface detector array is saturated (3 EeV). At a given energy, the geomagnetic effect is shown to induce a pseudo-dipolar pattern at the percent level in the declination distribution that needs to be accounted for before performing large scale anisotropy searches.

**Keywords:** geomagnetic field, energy estimate, large scale anisotropy, Pierre Auger Observatory

## 1 Introduction

The development of extensive air showers in the Earth's atmosphere is influenced by the geomagnetic field, which acts on the charged particles in the shower. This results in broadening of the spatial distribution of the particles in the direction of the Lorentz force. Current empirical models, used in the reconstruction of the primary energy and other parameters for showers with zenith angle  $\theta < 60^\circ$  detected with the Surface Detector array of the Pierre Auger Observatory, assume a radial symmetry of the particle distribution in the plane perpendicular to the shower axis. The geomagnetic field induces a systematic effect on the energy estimate, depending on the angle between geomagnetic field and the shower direction. This effect is currently neglected in the measurement of the energy spectrum with the Pierre Auger Observatory based on showers with zenith angles smaller than  $60^\circ$ . This is reasonable since the magnitude of the effect is well below the statistical uncertainty of the energy reconstruction, which is of order 15% [1]. However, in the search for large scale anisotropies at the percent level it induces a modulation of the measured cosmic ray event rate [2], resembling a true dipolar asymmetry in the North-South direction. The local magnetic field vector is approximately time independent, so this effect has no influence on a large scale anisotropy search in the right ascension distribution of cosmic rays [3, 4]. An analysis of the geomagnetic effect in the framework of horizontal air showers can be found in [5, 6].

## 2 Influence of the geomagnetic field on extensive air showers

The primary interaction of a cosmic ray in the atmosphere is followed by a hadronic cascade generating the muonic and electromagnetic shower components. The shower muons are produced by the decay of charged pions and have a typical energy  $E_\mu$  of a few GeV. The production point of these muons is within tens of metres of the shower axis and their energy loss, mainly due to ionisation, is relatively small (about  $2 \text{ MeV g}^{-1} \text{ cm}^2$ ). Unlike the electrons in the electromagnetic cascade, muons are weakly scattered and a large fraction of them reaches the ground. The geomagnetic effect will be therefore dominated by the action of the Lorentz force on the shower muons. In this analysis we treat the geomagnetic field  $\mathbf{B}$  at the Pierre Auger Observatory site as a constant field

$$B = 24.6 \mu\text{T}, \quad D_B = 2.6^\circ, \quad I_B = -35.2^\circ, \quad (1)$$

$D_B$  and  $I_B$  being the field's declination and inclination.

### 2.1 Distortion of the shower symmetry

Using a simple toy model we aim at understanding the main features of the muon density distortion induced by the geomagnetic field. In the absence of this field and neglecting scattering processes, a relativistic muon of energy  $E_\mu$  and transverse momentum  $p_T$  that travels a distance  $d$  will have

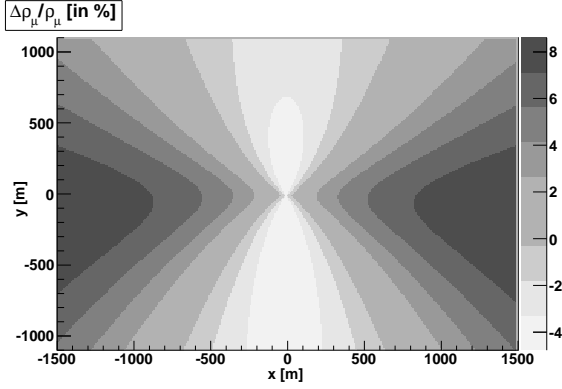


Figure 1: Relative changes of  $\Delta\rho_\mu/\rho_\mu$  in the transverse shower front plane due to the presence of the geomagnetic field, for a zenith angle  $\theta = 60^\circ$  and with the azimuth angle aligned along  $D_B + 180^\circ$ .

a radial deviation  $r$  from the shower axis given by

$$r \simeq \frac{p_T}{p_\mu} d \simeq \frac{cp_T}{E_\mu} d. \quad (2)$$

The deflection of a relativistic muon in the presence of a magnetic field with transverse component  $B_T$  can be approximated with

$$\delta x_\pm \simeq \pm \frac{ecB_T d^2}{2E_\mu}, \quad (3)$$

where the  $x$ -axis is oriented along the direction of the deflection. Given a muon density  $\rho_\mu(x, y)$  in the shower plane in the absence of the geomagnetic field, the corresponding density  $\bar{\rho}_\mu(\bar{x}, \bar{y})$  in the presence of the geomagnetic field is given by

$$\bar{\rho}_\mu(\bar{x}, \bar{y}) = \rho_{\mu+}(\bar{x} - \delta x_+, \bar{y}) + \rho_{\mu-}(\bar{x} - \delta x_-, \bar{y}), \quad (4)$$

neglecting a dependence of  $\delta x_\pm$  on  $x$  and  $y$ , which is only valid for a restricted range in  $r$ . Here we are interested in the shower size at  $r \simeq 1000$  m, which is used to estimate the primary energy [8]. Assuming a symmetry in the distribution of positive and negative muons, we can further simplify this equation to

$$\bar{\rho}_\mu(\bar{x}, \bar{y}) \simeq \rho_\mu(\bar{x}, \bar{y}) + \frac{(\delta x)^2}{2} \frac{\partial^2 \rho_\mu}{\partial \bar{x}^2}(\bar{x}, \bar{y}), \quad (5)$$

where we used  $\delta x = \delta x_+ = -\delta x_-$  and  $\rho_{\mu-} = \rho_{\mu+} = \rho_\mu/2$ . The geomagnetic field thus changes the muon density by a factor proportional to  $B_T^2(\theta, \varphi)$ . This term describes the azimuthal behavior of the effect, as verified in the next section by Monte Carlo shower simulations.

## 2.2 Observation of the distortion

We illustrate the relative change  $\bar{\rho}_\mu/\rho_\mu$  by shower simulations in the presence and in the absence of the geomagnetic field. A predominantly quadrupolar asymmetry is visible,

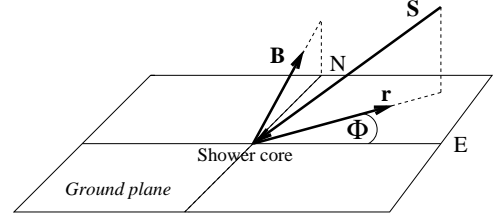


Figure 2: Definition of the polar angle  $\Phi$ , with respect to the shower core of a shower  $S$  and the magnetic East  $E$ .

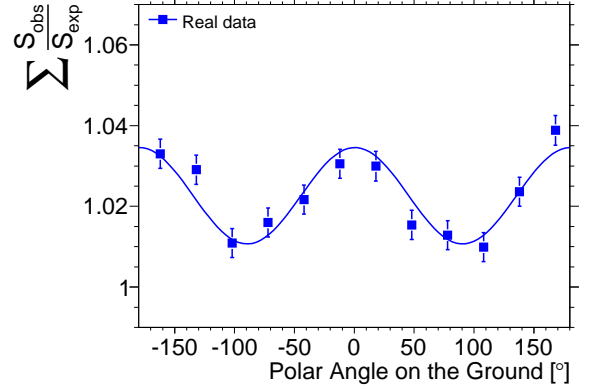


Figure 3: Ratio between observed and expected signal in the surface detectors (with radial distance  $r$  to the shower core larger than 1000 m) as a function of the polar angle  $\Phi$ . The solid line is a fit of a quadrupolar modulation.

corresponding to the separation of positive and negative charges in the direction of the Lorentz force (Fig. 1).

This effect is expected to manifest itself in a quadrupolar modulation of the surface detector signals as a function of the polar angle  $\Phi$ , defined with respect to the magnetic East as shown in Fig. 2. The ratio between observed and expected signal (which is calculated assuming radial shower symmetry) as a function of  $\Phi$  is shown in Fig. 3, drawn from approximately 30 000 showers with energies larger than 4 EeV, observed by the Pierre Auger Observatory until December 2010 and passing standard fiducial cuts [7]. A significant quadrupolar modulation of  $(1.2 \pm 0.2)\%$  is observed in the data. Its origin can be ascribed to the geomagnetic field, as was verified by an end-to-end Monte Carlo simulation, that was constructed to be similar to the real data in terms of shower energies and arrival directions. The quadrupolar amplitude in the case of simulations is  $(1.1 \pm 0.2)\%$  in the presence of the geomagnetic field (phase consistent with the real data case) and  $(0.1 \pm 0.2)\%$  in its absence. Details of this analysis can be found in [9].

## 3 Geomagnetic distortions of the energy estimator

The energy estimates of showers detected with the Surface Detector array are done in a three step procedure [8]. First,

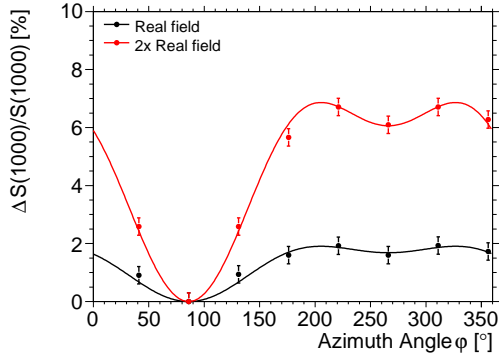


Figure 4:  $\Delta S(1000)/S(1000)$  (in %) as a function of the azimuth angle  $\varphi$ , at zenith angle  $\theta = 55^\circ$ .

the shower size  $S(1000)$  at 1000 m from the shower core is calculated, by fitting the lateral distribution function to the detector signals. Then the dependence of  $S(1000)$  on the zenith angle, arising from the attenuation of the shower in the atmosphere and from the surface detector geometry is quantified by applying the *Constant Intensity Cut* (CIC) method, resulting in the shower size  $S_{38}$  at reference zenith angle  $\theta = 38^\circ$ . The conversion of  $S_{38}$  to energy  $E$  is then achieved using a relation of the form  $E = AS_{38}^B$  which is calibrated using hybrid events that have an independent energy measurement from the Fluorescence Detector [1].

As predicted by the toy model above, the shower size  $S(1000)$  shifts proportionally to  $B_T^2 \propto \sin^2(\widehat{\mathbf{u}, \mathbf{b}})$ , the hat notation denoting the angle between shower direction  $\mathbf{u}$  and magnetic field direction  $\mathbf{b}$ . We verified this prediction by simulating sets of showers with fixed directions, each set containing 1000 showers simulated in the presence and in the absence of the geomagnetic field. The showers were generated with the AIRE program [10] and the hadronic interaction model QGSJET, simulating protons of 5 EeV. We find a systematic shift of the reconstructed  $S(1000)$  values, that follows the predicted azimuthal behavior (Fig. 4).

The zenithal behavior of the  $S(1000)$  shift depends on the muon distribution properties and cannot be predicted by the toy model. To obtain it by a Monte Carlo calculation, we created further sets of 1000 showers, for different zenith angles. The result is shown in Fig. 5, where the superimposed curve  $G(\theta)$  is an empirical fit of the data points. To obtain the pure zenithal dependency, the  $S(1000)$  shift was divided by  $\sin^2(\widehat{\mathbf{u}, \mathbf{b}})$ .

Placing the azimuthal and the zenithal dependence together, we arrive at a parametrisation of the geomagnetic shower size shift given by

$$\frac{\Delta S(1000)}{S(1000)}(\theta, \varphi) = 4.2 \times 10^{-3} \cos^{-2.8}(\theta) \sin^2(\widehat{\mathbf{u}, \mathbf{b}}). \quad (6)$$

Note that these results were obtained by simulating protons of 5 EeV. It is shown in [9] that the above parametrisation depends only weakly on energy, composition and the hadronic interaction model used in the simulations.

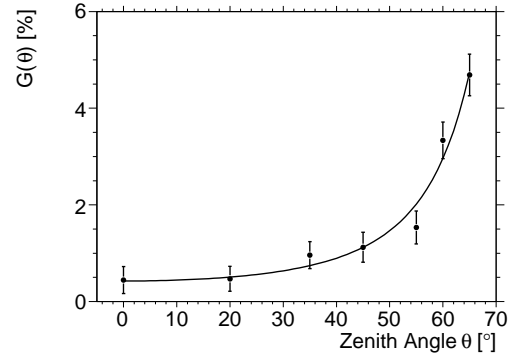


Figure 5:  $G(\theta) = \Delta S(1000)/S(1000) / \sin^2(\widehat{\mathbf{u}, \mathbf{b}})$  as a function of zenith angle  $\theta$ .

Part of the zenithal shift of  $S(1000)$  induced by the geomagnetic field is already corrected for by the CIC procedure, which assumes a uniform flux. By construction the CIC averages over the azimuthal variation. We therefore obtain the following correction formula that gives the reconstructed energy  $E$  in terms of the value  $E_0$  that is reconstructed if the effect of the geomagnetic field is not accounted for

$$E = \frac{E_0}{(1 + \Delta(\theta, \varphi))^B}, \quad (7)$$

with

$$\Delta(\theta, \varphi) = G(\theta) \left[ \sin^2(\widehat{\mathbf{u}, \mathbf{b}}) - \langle \sin^2(\widehat{\mathbf{u}, \mathbf{b}}) \rangle_\varphi \right] \quad (8)$$

where  $\langle \cdot \rangle_\varphi$  denotes the average over  $\varphi$ , taking the influence of the CIC procedure into account and  $B$  is one of the parameters used in the  $S_{38}$  to  $E$  conversion described above.

## 4 Consequences for large scale anisotropy searches

The influence of the geomagnetic effect on large scale anisotropy analysis is caused by the angular dependence of the energy estimate, that translates into a shift in the measured event rate at a fixed estimated energy.

### 4.1 Impact on the event rate

Above 3 EeV, the surface array has full acceptance, so the exposure is geometrical [7] and given by

$$\omega(\theta) \propto \cos(\theta) H(\theta - \theta_{\max}) \quad (9)$$

where  $H$  is the Heaviside step function that imposes a maximum observed zenith angle  $\theta_{\max}$ . The event rate at a given declination  $\delta$  and above an energy threshold  $E_{\text{th}}$  is obtained by integrating in energy and right ascension  $\alpha$

$$N(\delta) \propto \int_{E_{\text{th}}}^{\infty} dE \int_0^{2\pi} d\alpha \omega(\theta) \frac{dN(\theta, \varphi, E)}{dE} \quad (10)$$

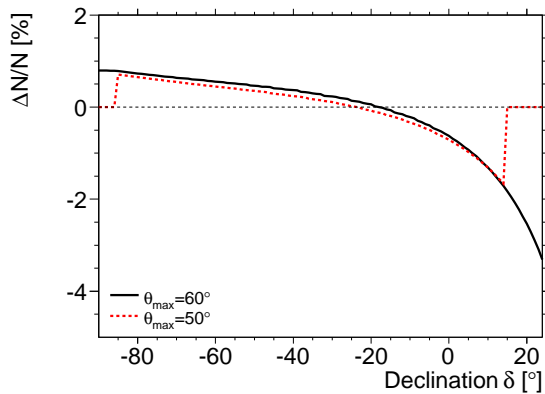


Figure 6: Relative differences  $\Delta N/N_{\text{corr}}$  as a function of the declination.

We assume that the cosmic ray spectrum is a power law, i.e.  $dN/dE \propto E^{-\gamma}$ . From Eqn. (7) it follows that if the effect of the geomagnetic field were not accounted for, the spectral distribution would have a directional modulation given by

$$\left(\frac{dN}{dE}\right)_0 \propto [1 + \Delta(\theta, \varphi)]^{B(\gamma-1)} \times E_0^{-\gamma}, \quad (11)$$

The event rate  $N_0(\delta)$  as a function of declination is then calculated using Eqn. (11) in Eqn. (10). The relative difference  $\Delta N/N$  is shown in Fig. 6 as a function of the declination, with spectral index  $\gamma = 2.7$ . It corresponds to the deviation from isotropy that would be observed above a fixed energy threshold if the geomagnetic effect were not accounted for in the reconstruction of the energy. The pattern displayed in Fig. 6 is similar to that produced by a dipole anisotropy in North-South direction with an amplitude at the percent level.

## 4.2 Impact on dipolar anisotropy searches

To study the effect of the modulation in the energy estimator on dipolar anisotropy searches we drew samples of simulated data from the “uncorrected” event rate  $N_0(\delta)$ . For the dipolar anisotropy search we used the method described in [11], which is adapted to a partial sky coverage. The results of the reconstructed dipolar amplitudes for 1000 mock data sets are shown in Fig. 7, for two different sample sizes. The expected isotropic distribution is plotted in the curves with solid lines. Its analytical expression is derived in [9]. For  $N = 300\,000$  events, we find a strong deviation from the expected distribution. The condition  $N = 32\,000$  is the number of events, for which the mean of the histogram is of the same order as the mean noise amplitude from the isotropic distribution.

In addition to having a non-isotropic amplitude distribution, the reconstructed dipole is preferentially oriented towards the South. For  $N = 32\,000$  events, the declination distribution is shown in Fig. 8.

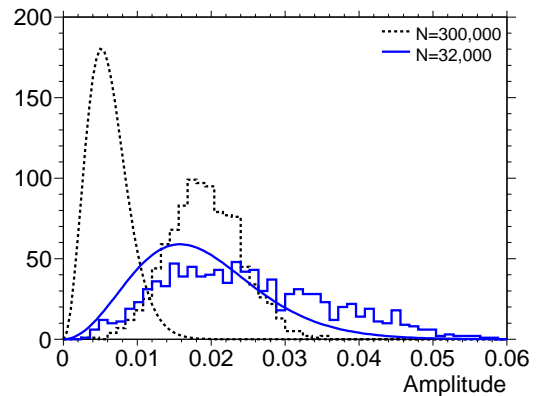


Figure 7: Two distributions of dipolar amplitudes reconstructed from arrival directions of mock data sets whose event rate is distorted by the geomagnetic effect, and their expected isotropic distribution.

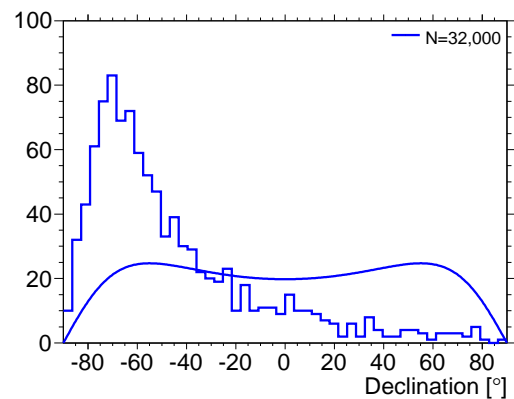


Figure 8: Distribution of reconstructed dipolar declinations and expected isotropic distribution.

## References

- [1] R. Pesce, for The Pierre Auger Collaboration, paper 1160, these proceedings
- [2] A. Ivanov *et al.*, JETP Letters, 1999, **69**: 288
- [3] The Pierre Auger Collaboration, Astropart. Phys., 2011, **34**: 627
- [4] H. Lyberis, for The Pierre Auger Collaboration, paper 0493, these proceedings
- [5] M. Ave, R. A. Vazquez, and E. Zas, Astropart. Phys., 2000, **14**: 91
- [6] H. Dembinski *et al.*, Astropart. Phys., 2010, **34**: 128
- [7] The Pierre Auger Collaboration, Nucl. Instr. and Meth. A, 2010, **613**: 29
- [8] The Pierre Auger Collaboration, Phys. Rev. Lett., 2008, **101**: 061101
- [9] The Pierre Auger Collaboration, in preparation
- [10] S.J. Sciutto, Proc. 27th ICRC, Hamburg, Germany, 2001, **1**: 237
- [11] P. Billoir, O. Deligny, JCAP, 2008, **02**: 009